Reinforcement Learning Assisted Beamforming for Inter-cell Interference Mitigation in 5G Massive MIMO Networks

Aidong Yang, Ph.D
Telecom Artificial Intelligence Lab
AsiaInfo Technologies
Beijing, China
yangad@asiainfo.com

Xinlang Yue*
Telecom Artificial Intelligence Lab
AsiaInfo Technologies
Beijing, China
yuexl3@asiainfo.com

Ye Ouyang, Ph.D
Telecom Artificial Intelligence Lab
AsiaInfo Technologies
Beijing, China
ye.ouyang@asiainfo.com

ABSTRACT

Beamforming is an essential technology in the 5G massive multiple-input-multiple-output (MMIMO) communications, which are subject to many impairments due to the nature of wireless transmission channel, i.e. the air. The inter-cell interference (ICI) is one of the main impairments faced by 5G communications due to frequency-reuse technologies. In this paper, we propose a reinforcement learning (RL) assisted full dynamic beamforming for ICI mitigation in 5G downlink. The proposed algorithm is a joint of beamforming and full dynamic Q-learning technology to minimize the ICI, and results in a low-complexity method without channel estimation. Performance analysis shows the quality of service improvement in terms of signal-to-interference-plus-noise-ratio (SINR) and computational complexity compared to other algorithms.

CCS CONCEPTS

• **Networks** → **Wireless access points, base stations and infrastructure**; • **Computing methodologies** → *Model development and analysis*; • **Theory of computation** → **Reinforcement learning**.

KEYWORDS

5G, massive MIMO, Reinforcement Learning, Inter-cell Interference

1 INTRODUCTION

MMIMO technology in 5G is a competent solution that significantly improves system capacity, signal coverage and spectral-efficiency by configuring hundreds of antenna elements (AEs) at base station (BS) to shape effective beamforming [1][7]. However, the quality of MMIMO beamforming depends on accurate channel state information (CSI), pilot contamination and ICI estimation [25]. Moreover, the MMIMO beamforming complexity becomes a challenge as the number of AEs at BS increases. Therefore, it is necessary to explore an effective and efficient beamforming method for the ICI mitigation with low-power and low-complexity [15].

In recent years, the accurate MMIMO beamforming has attracted extensive researches [25][15][24][12][8], which are almost in two main directions: with and without CSI. Hybrid beamforming [25][15][24] is the representative of the former. It aims to reduce the expense of radio frequency (RF) chains and decrease the complexity of beamforming compared to the conventional methods [7], but it needs to update beams frequently when pilots are received continually at BS. A smart pilot assignment scheme, which is effective to mitigate interference but aims at a single cell, is proposed in [24] to reduce pilot contamination by smartly assigning orthogonal pilots to users. The latter mainly includes first Monte Carlo (MC) method, which searches the optimal beamforming parameters but suffers from increasing computational complexity, and second deep learning (DL) methods. One of them is reported in [8] to research the characters of wireless spatial channels and explore preferable pilot assignments for better channel estimation and beamforming, but DL methods require training algorithmic model beforehand and time-consuming sample data collection.

In this paper, an RL assisted full dynamic beamforming method is developed to efficiently acquire the optimal beamforming parameters in MMIMO system to address ICI issues. We fully consider the micro- and macro-cell multi-path transmission channels which present radio features with high user density and tranffic loads focusing on pedestrian and vehicular users (Dense Urban-eMBB) scenarios [1][7][24], such as buildings, mountains and rivers, where the distribution of user equipments (UEs) change infrequently, these factors significantly impact coverage. To get the optimal beamforming, firstly, we utilize Poisson Point distribution model to estimate the occurrences of UEs in the target cells with a long-term data statistical analysis; Secondly, we apply RL algorithm to fast search through huge volumes of parameters and obtain optimal values. Lastly, we send the optimal parameters into the BS beamforming simulator for the best SINR.

In summary, the main contribution of this work includes:

- The proposed RL assisted full dynamic beamforming method does not require channel estimation and does decrease the computational complexity compared to traditional methods.
- The RL model outputs the optimal beamforming parameter, considers the distribution of UEs in different scenarios and multi-cell ICIs.
- The RL model is of sample efficiency and takes much less time in adapting to the environment change.

The rest of the paper is organized as follows. In Section 2, related works on RL-based ICI mitigation are presented. The system model and our proposed Dynamic-Q learning scheme are presented in Section 3 and 4. In Section 5, simulation results are presented and the conclusion follows in Section 6.

2 RELATED WORK

ICI control is a key issue in 5G MMIMO systems, intensive research has been carried out to address it. Surveys have been carried out on ICI mitigation techniques in 5G downlink networks [3][19], on ICI coordination techniques in OFDMA-based cellular networks [6] and

*Corresponding author.

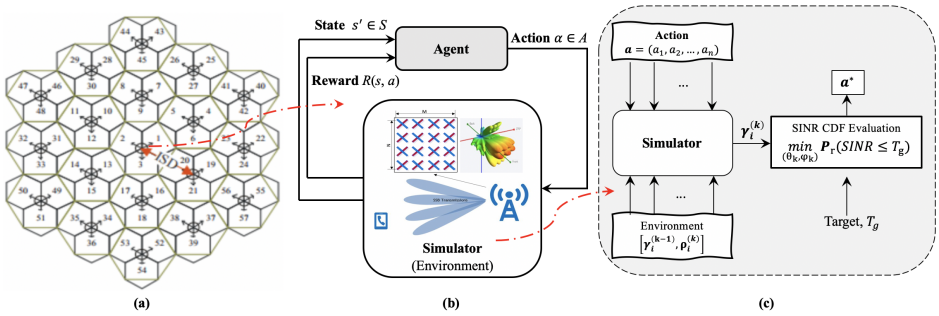

Figure 1: Illustration of the proposed RL-based beamforming (b) for MMIMO sysyems and the network layout (a) of 5G dense Urban-eMBB cells, in which the BS of target small cell #0 with $N_0(k)$ mobile users chooses the optimal beamforming $a_0^{*(k)}$ (c) to mitigate interference from the neighboring N_{cell} small cells at time slot k, and $N_0(k)$ users return estimated SINRs $\gamma_N(k)$ to the BS.

on ICI mitigation techniques in OFDMA-based cellular networks and LTE [11].

RL-based approaches have been extensively applied in ICI mitigation problem. For instance, a Q-learning-based power control scheme formulates the ICI coordination issue as a cooperative multi-agent control problem to improve the performance of the cellular systems is proposed in [4]. An RL-based power control scheme for ultra-dense small cells to improve network throughput and save energy consumption is presented in [23], in which BS select downlink transmit power to manage interference. A dynamic RL-based ICI coordination algorithm as developed in [18] smartly offloads traffic to open access picocells and then improves the system throughput.

3 SYSTEM MODEL

ICI is caused by multiple sources transmitting signals with the same subcarrier and received by a receiver. A user receives signals from the serving cell and neighboring cells but at different power levels due to the pathloss.

3.1 AOA-based Beamforming

The angle-of-arrive (AOA) based beamforming is usually used in 5G MMIMO system, where the BS is configured with an antennas array composed of W AEs, and M AEs are arranged in a row and L AEs in a column [7]. In RF, the BS shapes beamforming for the k^{th} UE by configuring weights on AEs according to AOA $\langle \theta_k, \varphi_k \rangle$ [2], where θ_k is the horizontal azimuth and φ_k is the vertical angle of the k^{th} UE. The weights on the i^{th} AE in a row can be represented as

$$\omega_{ik} = e^{-j2\pi i d_h \sin\theta_k}, w_{ik} \in C^{1*M} \tag{1}$$

where d_h is the row AE distance. And the l^{th} AE in the column can be obtained by

$$\xi_{lk} = e^{-j2\pi l d_v \cos\varphi_k}, \xi_{lk} \in C^{L*1} \tag{2}$$

where d_v is the column AE distance. From (1) and (2), the final beamforming weights for the k^{th} UE can be derived by

$$\prod_k = \Psi_k \Omega_k \tag{3}$$

where $\Omega_k = [\omega_{1k}, \omega_{2k}, \ldots, \omega_{Mk}]$, $\Psi_k = [\xi_{1k}, \xi_{2k}, \ldots, \xi_{Lk}]^T$.

Since the final weights in (3) depends on $\langle \theta_k, \varphi_k \rangle$, the implement complexity for $\langle \theta_k, \varphi_k \rangle$ estimation gets high as the perfect CSI needed, which is usually affected by ICI.

3.2 Search-based Beamforming

To mitigate the ICI with a low-complexity, a search-based beamforming algorithm is reported in [2], which uses MC to search the optimal weights rather than AOA estimation in (3). In MC beamforming, the best weights are obtained by searching $\langle \theta_k, \varphi_k \rangle$ in all possible angles to minimize the ICI, i.e.

$$\begin{aligned} \langle \theta_k^*, \varphi_k^* \rangle \longleftarrow \arg \min_{\langle \theta_k, \varphi_k \rangle} P_r(SINR < T_g | h_j^{(k)}, \rho_j^{(k)}) \\ s.t. -\pi \le \theta_k, \varphi_k \le \pi \end{aligned} \tag{4}$$

where P_r is the probability of SINRs weaker than the target T_g given the channel $h_j^{(k)}$ and UE density $\rho_j^{(k)}$, and the SINR in (4) for the i^{th} UE located on the j^{th} cell can be expressed by [2]

$$SINR_{i,j} = \frac{p_{i,j} \varsigma_{i,j}^{-\nu}}{N_0 B + \sum_{k=1, k\neq j}^{N} p_k \varsigma_k^{-\nu}} \tag{5}$$

where ν is the path-loss exponent, $p_{\cdot j}$ is the transmit power of the serving enode B_j, N is the number of neighboring enode B_s, p_k is the transmit power from B_s, $\varsigma_{\cdot j}$ is the distance of the UE to the serving station, ς_k is the distance of the UE to each of the neighboring stations, and $N_0 B$ is the background noise with N_0 the thermal noise and B the system bandwidth.

According to [14], the UE density $\rho_0^{(k)}$ in (4) is assumed to follow the independently and identically distributed two-dimensional Poisson point process. The number of users $N_0^{(k)}$ of the target cell with area φ_0 is given by

$$Pr\{N_0^{(k)} = \lambda | \varphi_0\} = \frac{(\rho_0^{(k)} \varphi_0)^\lambda}{\lambda!} e^{-\rho_0^{(k)} \varphi_0} \tag{6}$$

From (4) to (6), the optimal parameters $\langle \theta_k^*, \varphi_k^* \rangle$ can be found, and the best weight $\prod_k$ can be derived by substituting (4)-(6) into (3).

4 THE PROPOSED REINFORCEMENT LEARNING ASSISTED BEAMFORMING

In this section, we propose an RL assisted full dynamic beamforming method to mitigate ICI and reduce the system complexity. Each BS exploits the user SINRs in a dense Urban-eMBB transmission environment and estimates probability density function (PDF) of users' occurences to achieve an optimal beamforming solution via trial without knowledge of the network and transmission channel.

4.1 RL-based Beamforming

In the RL-based beamforming process as shown in Figure 1(a) (b), the BS in the target cell estimates the probability density $\rho_0^{(k)}$ of users' occurences in the target small cell #0 by a long-term data statistical analysis in (6) at time slot k. Once all served users send SINRs $\gamma^{(k-1)}$ at the time slot $(k-1)$ to the BS, the state $[\rho_0^{(k)}, \gamma^{(k-1)}]$ observed by the BS at the time slot k is obtained, and then an RL-based beamforming algorithm is applied for searching the optimal parameters for the ICI mitigation and coverage optimization.

Following Algorithm 1, we formulate the beamforming optimization problem under the MMIMO system context as an RL problem and therefore provide a dynamic Q-learning scheme to address the issue.

The objective is to approach a desire target SINR state: s_0. It covers the probability in (4) of average regional SINR given by the simulator and guided by selected action a_t. $A = \{a_i\}_{i=0}^{n-1}$ and $S = \{s_i\}_{i=0}^{m-1}$ are the sets of agents' actions and states respectively. The environment (Figure 1(c)) grants the agent a reward $r_{s,a}$ after the latter takes an $a \in A$ when it is in $s \in S$ at discrete time t.

Formally, we denote the state-action value function, the expected discounted reward, as $Q(s, a)$. In the table $\mathbf{Q} \in R^{m \times n}$, we use notation [10] $Q(s, a) \triangleq [\mathbf{Q}]_{s,a}$ and update entries by:

$$Q(s, a) \leftarrow Q(s, a) + \alpha[r_{s,a} + \delta \max_{a'} Q(s', a') - Q(s, a)] \quad (7)$$

where $\alpha : 0 < \alpha < 1$ is the learning rate and $\delta : 0 < \delta < 1$ is the *discount* factor and determines the importance of future rewards. s' and a' are the next state and action, respectively.

An *episode* is a period of time in which an interaction between the environment and the agent takes place. Here, the episode is of (at most) τ transitional discrete times. During an episode $i : i \in \{0, 1, \ldots, \zeta\}$, the agent makes decision to maximize the effects of actions decided by itself. To achieve this goal, we apply the ϵ-greedy learning strategy to balance the exploration and exploitation, where $1 - \epsilon : 0 < \epsilon < 1$ is the exploration rate and serves as the threshold probability to select a random $a \in A$, as opposed to selecting an action based on exploitation. To add randomness, the ϵ increases in every episode from ϵ_{min} until it reaches a preset upper bound.

The S space is constructed by partitioning the range of processed cumulative distribution function (CDF), which is the probability of users with SINR under the given T_g in (4). The components of A space is shown in Table 1. Through a finite series of $a \in A' := A - \mathbf{C}$ (will be discussed later), the agent attempts to approach s_0 in response to simulated s_i at step t within an episode.

4.2 Reward Signals

4.2.1 Reward Design with Q-initialization.

Table 1: Learning Parameters

Parameter	Value
Learning rate α	0.01
Reward decay rate δ	0.9
Minimum exploration rate ϵ_{min}	0.9
Number of episodes ζ	22
Each episode duration τ	40
Number of states	30
Number of actions	855

As discussed in [13], reward signals in our simulation environment are crucial to the RL Markov decision process (MDP) since agent are expected to learn the optimal policy under industrial criteria.

Since adding additional rewards follows the policy invariance [13], the reward function $r(s, a)$ within our problem setting consists of two main parts:

$$r(s, a) = r(s_0, a)_{goal} + r(s, a)_{inter} \quad (8)$$

$r(s_0, a)_{goal}$ is given to the agent if s_0 is approached and $r(s, a)_{inter}$ works as intermediate reward in the training process when $s \neq s_0$.

We aim at constructing reward shaping for $r(s, a)_{inter}$ using potential-based method to help guide the agent in MDP, the potential-based shaping function is defined as [13]:

Definition 1. *Let any S, A, δ and any shaping reward function $F : S \times A \times S \rightarrow \mathbb{R}$ in MDP be given. F is **potential-based** if there exists a real-valued function $\Phi : S \rightarrow \mathbb{R}$ s.t.*

$$F(s, a, s') = \delta\Phi(s') - \Phi(s) \quad (9)$$

for all $s \neq s_0, s' \in S, a \in A$.

Therefore, based on the results in [13], such an F can guarantee consistency with the optimal policy that agent learned. Luckily, there is no need to construct the shaping function from scratch [22], since the design of F is equivalent to the initialization of $[\mathbf{Q}]_{s,a}$.

Suppose the optimal policies learnt in our model with and without potential-based F are π' and π, respectively. Let initial Q function of π be $Q(s, a) = Q_0(s, a)$ with shaping rewards $\delta\Phi(s') - \Phi(s)$, and initial Q function of π' be $Q'(s, a) = Q_0(s, a) + \Phi(s)$ with no shaping rewards.

By (7), we have the update error:

$$\begin{cases} Q_{error} = r_{s,a} + \delta\Phi(s') - \Phi(s) + \delta \max_{a'} Q(s', a') - Q(s, a) \\ Q'_{error} = r_{s,a} + \delta \max_{a'} Q'(s', a') - Q'(s, a) \end{cases} \quad (10)$$

and now insert ΔQ and $\Delta Q'$, the difference between current and initial values of Q and Q' respectively, into the update error:

$$\begin{cases} \Delta Q(s, a) = Q(s, a) - Q_0(s, a) \\ \Delta Q'(s, a) = Q'(s, a) - Q_0(s, a) - \Phi(s) \end{cases} \quad (11)$$

we have

$$\begin{aligned} Q_{error} &= r_{s,a} + \delta\Phi(s') - \Phi(s) + \delta \max_{a'}(Q_0(s',a') + \Delta Q(s',a')) \\ &\quad - Q_0(s,a) - \Delta Q(s,a) \\ &= r_{s,a} + \delta \max_{a'}(\Phi(s') + Q_0(s',a') + \Delta Q(s',a')) \\ &\quad - Q_0(s,a) - \Delta Q(s,a) - \Phi(s) \\ &= r(s,a) + \delta \max_{a'} Q'(s',a') - Q'(s',a') \\ &= Q'_{error} \end{aligned} \tag{12}$$

Therefore, we investigate on the relation between r_{inter} and $Q_0(s,a)$ to decide the form of r_{inter}. In the MDP problem setting [21], the discounted return from time step t is $G_t = \sum_{k=0}^{\infty} \delta^k r_{t+k+1}$, and since $\delta \in (0,1)$, if r_{inter} is formed as a bounded series based on the distance from s_0 to s_i: $r(s,a)_{inter} \leq r_{bound}$, where $r_{bound} \leq 1$, we have

$$\begin{aligned} G_t &= \sum_{k=0}^{\infty} \delta^k r_{t+k+1} \\ &\leq \sum_{k=0}^{\infty} \delta^k r_{bound} \\ &\leq r_{bound} \sum_{k=0}^{\infty} \delta^k \\ &= \frac{r_{bound}}{1-\delta} \end{aligned} \tag{13}$$

then for optimal policy π' [21]

$$\max_a Q^{\pi'}(s,a) = E[G_t] \leq r_{goal} \tag{14}$$

we know r_{inter} and r_{goal} satisfy:

$$\frac{r_{bound}}{1-\delta} \leq r_{goal} \tag{15}$$

(15) gives an explicit gap between the two parts of $r(s,a)$ and also directly influence the following initialization of $Q_(s,a)$.

4.2.2 *Q-initialization Setting.*

We rewrite the initial Q table of policy π' and the final converged table as $Q_0^{\pi'}$ and $Q_{final}^{\pi'}$ respectively. By (7),

$$\begin{aligned} Q^{\pi'}(s,a) &\leftarrow Q_0^{\pi'} + \alpha(r_{bound} + \delta Q_0^{\pi'} - Q_0^{\pi'}) \\ &= Q_0^{\pi'} + \alpha(1-\delta)(Q_{final}^{\pi'} - Q_0^{\pi'}) \end{aligned} \tag{16}$$

we can derive that

$$Q_0^{\pi'} > Q_{final}^{\pi'} = \frac{r_{bound}}{1-\delta} \tag{17}$$

to guarantee the convergence of the model update. And under the Q-learning scheme, (17) always provide chances of exploration for actions that have not been attempted.

In this end, we define reward signals for $r(s,a)$ as follows:

$$r_{s_i,a} \triangleq \begin{cases} -\frac{e^{0.1\cdot(i-2)}}{e^{2.8}+1} & s_i \geq s_2 \\ -\frac{0.01}{e^{2.8}+1} & s_i = s_1 \\ \frac{e^{0.2\cdot(30-i)}}{e^{2.8}+1} & s_i = s_0 \end{cases} \tag{18}$$

and set $r_{bound} = -\frac{0.01}{e^{2.8}+1}$ from (18) to follow the conditions we derived in (13), (15). Therefore, we can initialize the Q function as $[\mathbf{Q}]_{s,a} := \mathbf{0}_{|S|\times|A|}$ to satisfy (17).

4.3 Dynamic Q-Learning Algorithm

Considering the computational and equipment cost in MMIMO system, the delaying effect of reward should be minimized. Then after each step t, we use twice ϵ-greedy strategy, the controller to help avoid the action that is unrelated to s_0 to dynamically shrink the A space in order to make up for the delay in (18). Therefore, the controller plays a highly efficient role as penalty signal in our reward and serves as a reinforced mechanism to assist the selection. The upper bound of the time complexity for the Dynamic Q-learning method is in $O(mn)$ [9].

For a total of at most n trials in ζ episodes with a fixed initial environmental CDF, the algorithm 1 will stop training the agent once s_0 is approached rather than continuing the process due to the reward signals design in our model:

Controller **C**: As shown in Algorithm 1, controller **C** will shrink the action space related to s in every step t based on double ϵ-greedy principle. This operation enables the optimal action selection with higher and higher probability as t goes on.

Algorithm 1 Optimal Action Selection Control

Input: Initial CDF state s_{init} and target state s_0.
Output: Optimal a to approach s_0 during episode i.

Define customized S, A, ϵ and δ.
Initialize $\mathbf{C} := \{\}$, $\boldsymbol{Q} := \mathbf{0}_{|S|\times|A|}$, $i := 0$
Initialize $s := s_{init}$, $t := 0$
repeat
  while $t < \tau$ **do**
    $\epsilon := \max_{a'}(\epsilon_{min}, \epsilon_{min} + \delta \cdot t/(\tau \cdot \zeta))$
    Sample $k_1, k_2 \sim \mathcal{U}(0,1)$
    if $k_1 \leq \epsilon$ **then**
      if $k_2 > \delta(1-\epsilon)$ **then**
        Select $a \in A - \mathbf{C}$, $a = \arg\max_{a'} Q(s,a')$
      else
        Select $a \in A$, $a = \arg\max_{a'} Q(s,a')$
      end
    else
      Select $a \in A - \mathbf{C}$ randomly
    end
    Perform a in the simulator and obtain $s', r(s,a)$
    Update the entry $Q(s,a)$ as in (7)
    $s \leftarrow s'$, $t \leftarrow t+1$
    if $s \neq s_0$ **then**
      Append a in $\mathbf{C}$
    else
      Early stopping
      return a
    end
  end while
until $s = s_0$ otherwise proceed to episode $i+1$

Table 2: Environment Components

Simulation Parameter	Value	Simulation Parameter	Value
Antenna 3dB-Bandwidth in Azimuth (°)	15 ∼ 110	Number of Observed UEs K_0	100
Antenna 3dB-Bandwidth in Elevation (°)	0 ∼ 30	Receiver Bandwidth (MHz)	20
Antenna Tilt Angle (°)	-3 ∼ 15	Receiver Height (m)	1.5
Carrier Frequency (GHz)	4	MM Array Type	URA
Height of BS (m)	25	MM Array Size	8×8
Transmit Power (dBm)	44	MM Mechanical Downtilt	15

Reward $r_{s,a}$: (18) guarantees the agent learns a global optimum, our target action, instead of continuously jumping on some local optimum for meaningless rewarding [5].

Reward signals and controller **C** attempt to guide the agent by avoiding redundant scoring and long term penalties. The agent itself continuously updates the learning policy under the guidance of both them.

4.4 Other Existing Methods

For not too large $S \times A$ space defined in Section 4.1, MC Exhaustion Algorithm often serves as a baseline solution for the problem in section 3. It requires testing on all possible $a \in A$ to ensure the best action among space A.

Therefore, we apply classical model-free RL methods: Q-learning (off-policy) and Sarsa (on-policy) [21] in this problem setting. They differ mainly in the Q function updating style, while Q-learning holds (7), Sarsa follows the update below:

$$Q(s,a) \leftarrow Q(s,a) + \alpha[r_{s,a} + \delta Q(s',a') - Q(s,a)] \tag{19}$$

Parameters for these models are set the same as in Table 1. Unsurprisingly, off-policy based methods are superior to on-policy methods [21] in the experiment discussed later.

With the experience gained from Algorithm 1, Algorithm 2 is proposed to test the trained agent's policy with any randomized given s_{init}.

Algorithm 2 Evaluation Algorithm

Input: Target state s_0 and $\boldsymbol{Q}$ from Algorithm 1.
Output: Optimal a, target s with rewards for Z episodes.

1: Load the experienced $\boldsymbol{Q} := [\mathbf{Q}]_{s,a}$, $z := 0$
2: **repeat**
3: Randomize s_{init} with $(s, a, r_{s_{init}}, t)_z := (0,0,0,0)_z$
4: Choose $a = \arg\max_{a'} Q(s_{init}, a')$
5: Perform a in the simulator and obtain $s', r_{s_{init}}, t$
6: Update $(s := s', a, r_{s_{init}}, t)_z$
7: $z \leftarrow z + 1$
8: **until** $z = Z$

5 SIMULATIONS AND DISCUSSIONS

To thoroughly investigate the performance of the proposed RL assisted full dynamic beamforming method and validate the effectiveness of the theoretical analysis previously, we present statistical results of SINRs and computational complexity of the proposed algorithm compared to other industrial methods. We implement Algorithm 1 within the environment below with preset parameters shown in both Table 1 and Table 2.

5.1 Environment Setting

The simulation is based on the guidelines defined in [17] for evaluating 5G radio technologies in an urban macro-cell test environment which presents radio channel with high user density and traffic loads focusing on pedestrian and vehicular users (Dense Urban-eMBB) [16]. As shown in Figure 1(a), the layout consists of 19 sites placed in a hexagonal layout, each with 3 cells, and the inter-site distance (ISD) is 200m. The visualize SINR for the simulation scenario using the Close-In propagation model [20], which models path loss for 5G urban micro-cell and macro-cell scenarios. This model produces an SINR map that shows reduced interference effects compared to the free space propagation model.

5.2 Computational Complexity

The agent learns from the environment for 1000 epochs of all randomized s_{init} and stores policy experience in the Q-table described in Algorithm 1. In this stage, our model performs faster and more stable than other methods mentioned above. We utilize three following metrics to help compare:

Normalized Iteration Expectation $\mathcal{I}_E$: it indicates the scaled steps expectation to approach s_0 in 1000 epochs of training.

Computational Efficiency (CE) $\mathcal{E}_*$: we define the ratio below to reflect computational cost saving:

$$\mathcal{E}_* \triangleq \frac{\mathcal{I}_\text{E} \text{ for Baseline MC}}{\mathcal{I}_\text{E} \text{ for method } i} \tag{20}$$

where $i \in$ {Dynamic Q, Q-learning, Sarsa}.

Reward Scoring: This metric indicates how Dynamic Q method is different from other methods in fastness and convergence when achieving reward.

Figure 2(a) displays the $\mathcal{I}_E$ with standard deviation, which implies stability in 1000 epochs, of how Dynamic Q model acts differently from Q-learning, Sarsa and MC. It takes the lowest normalized $\mathcal{I}_E$ needed to meet s_0 with the highest computational efficiency $\mathcal{E}_*$ (highlighted stars) and even doubles $\mathcal{E}_*$ compared to the baseline MC. (b) indicates the agility of our model in adapting to the environment. Given randomized s_{init}, the 95% confidence interval shadow indicates within 1000 epochs of training, the range and convergence rate of reward scoring for Dynamic Q model differ from other RL methods. Our model is able to fully train its agent in 10 episodes (without early stopping) with robustness and obtain

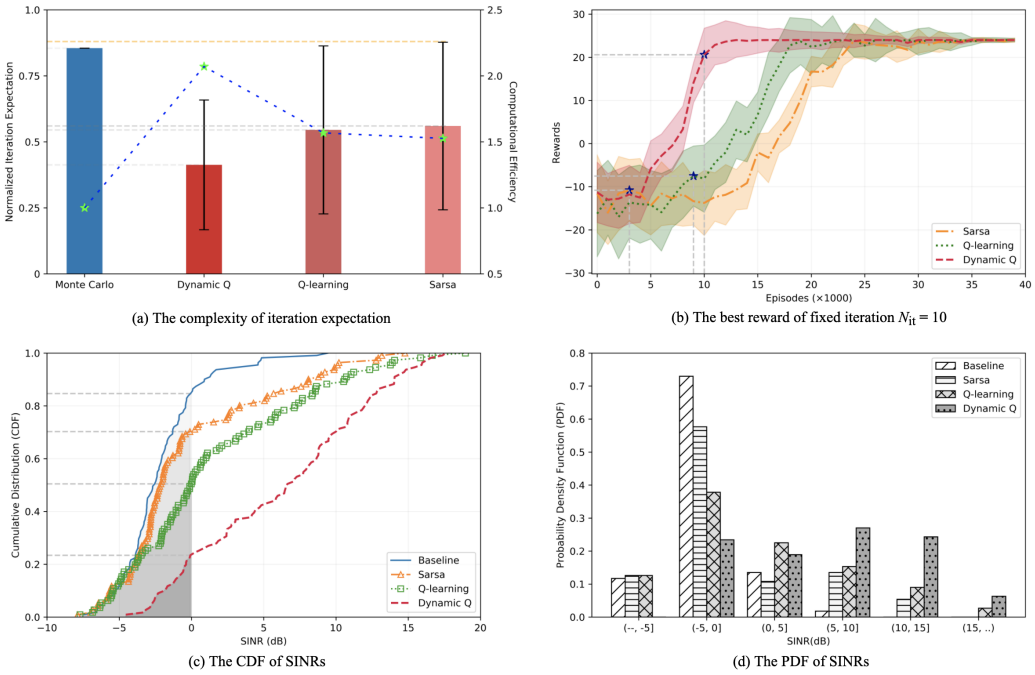

(a) The complexity of iteration expectation

(b) The best reward of fixed iteration $N_{\text{it}} = 10$

(c) The CDF of SINRs

(d) The PDF of SINRs

Figure 2: Comparison of computational complexity and SINR improvements of the proposed Dynamic Q algorithm with other industrial methods: MC (Baseline), Q-Learning and Sarsa. (a) shows the total iteration number for the optimal parameters; (b) displays their best reward when the iterate number is fixed to $N_{\text{it}} = 10$, each point on the mean curve of rewards is averaged across 1000 epochs with random s_{init}, the shadow is the 95% confidence interval across 40 episodes of three models setting; (c) and (d) gives the CDF and PDF of their SINRs.
$W = 64, N_{cell} = 57, K_0 = 100$.

the highest reward while other methods are still unstable under the two criteria.

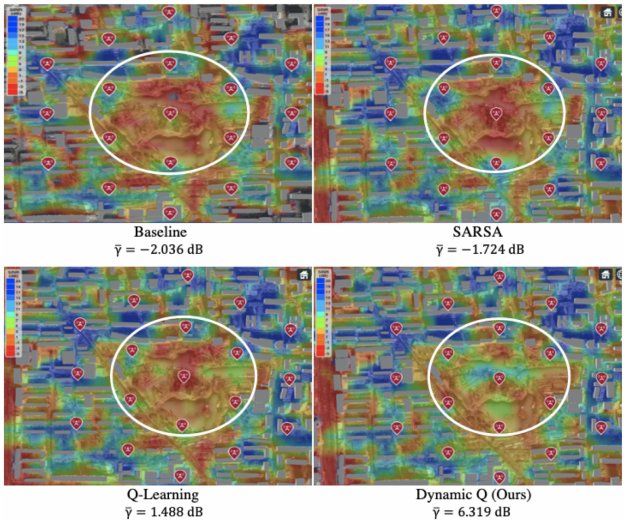

Figure 3: The average SINRs of different RL-based ICI mitigation algorithms in 5G MMIMO system, with parameters fed from Figure 2(b). White circles are ROI.
$W = 64, N_{cell} = 57, K_0 = 100$.

5.3 SINR Performance

We show our model's shifting effect on SINR coverage in Figure 2(c)(d) compared to other methods. With the optimal parameters derived from four models, respectively, within 10 episodes in (b) and sent into the simulator, (c) indicates ours is of the smallest weak SINR coverage that is lower than 0dB. Dynamic Q model sufficiently shift the distribution towards strong SINR direction, it enlarges the SINR coverage larger than 0 dB to over 50% of the total population in the region of interest (ROI). Specifically, (d) discloses that our model has the smallest probability density of users with weak SINR, for example, when SINR $\in (-5, 0]$, the probability is 23% with Dynamic Q model while it is 74%, 58%, 38% with the rest methods, respectively.

Figure 3 displays the application when the optimal action is sent into the simulator of different models in 10 training episodes. The Dynamic Q model is of the best average SINR of $\bar{\gamma} = 6.319$ dB in the ROI among all models.

In Table 3, we compare the average SINRs, across 6 different scenarios, for Dynamic Q model against MC, SARSA, and Q-Learning with parameters fed from Figure 2(b). It is clear that Dynamic Q model improves the UE SINRs across 6 different environments, particularly on the comparison with MC, we achieve the average SINR improvements of around 8.3 dB, 10.4 dB, 12.2 dB 11.2 dB and 11.8 dB, respectively.

Table 3: Application Scenarios

BS location		RL-based ICI mitigation algorithms			
Longitude	**Latitude**	**MC**	**Sarsa**	**Q-learning**	**Dynamic Q**
116.395659	39.959522	-2.036	-1.724	1.488	6.319
117.212147	39.161901	-4.732	-2.543	0.563	5.783
111.713038	40.832723	-7.931	-3.472	-1.239	4.374
111.710787	40.832027	-6.293	-2.174	0.897	4.978
111.709219	40.837586	-6.517	-2.573	1.296	5.381

6 CONCLUSION

In this paper, we propose an RL (i.e. Dynamic Q-learning) assisted full dynamic beamforming algorithm for the ICI mitigation in 5G MMIMO systems. This algorithm mitigates the ICI and reduces the computational complexity of the BS without knowledge of the network and transmission channel. Simulation results show the implement complexity is lower and UE SINRs is significantly improved compared to other industrial methods. For example, in the dense Urban-eMBB scenario, the probability of weak SINRs in the target cell is about 60% lower and computational complexity is reduced by more than 50% compared to the benchmark.

REFERENCES

[1] Emil Björnson, Erik G Larsson, and Thomas L Marzetta. 2016. Massive MIMO: Ten myths and one critical question. *IEEE Communications Magazine* 54, 2 (2016), 114–123.

[2] Joy Iong-Zong Chen, Bo Hueng Lee, and Wen Bin Wu. 2018. Performance evaluation of BER for an Massive-MIMO with M-ary PSK scheme over Three-Dimension correlated channel. *Computers & Electrical Engineering* 65 (2018), 196–206.

[3] A Daeinabi, K Sandrasegaran, and X Zhu. 2012. Survey of intercell interference mitigation techniques in LTE downlink networks. In *Australasian Telecommunication Networks and Applications Conference (ATNAC) 2012*. IEEE, 1–6.

[4] Mariana Dirani and Zwi Altman. 2010. A cooperative reinforcement learning approach for inter-cell interference coordination in OFDMA cellular networks. In *8th International Symposium on Modeling and Optimization in Mobile, Ad Hoc, and Wireless Networks*. IEEE, 170–176.

[5] Dylan Hadfield-Menell, Smitha Milli, Pieter Abbeel, Stuart J Russell, and Anca Dragan. 2017. Inverse reward design. In *Advances in neural information processing systems*. 6765–6774.

[6] Abdelbaset S Hamza, Shady S Khalifa, Haitham S Hamza, and Khaled Elsayed. 2013. A survey on inter-cell interference coordination techniques in OFDMA-based cellular networks. *IEEE Communications Surveys & Tutorials* 15, 4 (2013), 1642–1670.

[7] Jakob Hoydis, Stephan Ten Brink, and Mérouane Debbah. 2013. Massive MIMO in the UL/DL of cellular networks: How many antennas do we need? *IEEE Journal on selected Areas in Communications* 31, 2 (2013), 160–171.

[8] Kwihoon Kim, Joohyung Lee, and Junkyun Choi. 2018. Deep learning based pilot allocation scheme (DL-PAS) for 5G massive MIMO system. *IEEE Communications Letters* 22, 4 (2018), 828–831.

[9] Sven Koenig and Reid G Simmons. 1993. Complexity analysis of real-time reinforcement learning. In *AAAI*. 99–107.

[10] Raghavendra V Kulkarni, Anna Förster, and Ganesh Kumar Venayagamoorthy. 2010. Computational intelligence in wireless sensor networks: A survey. *IEEE communications surveys & tutorials* 13, 1 (2010), 68–96.

[11] Raymond Kwan and Cyril Leung. 2010. A survey of scheduling and interference mitigation in LTE. *Journal of Electrical and Computer Engineering* 2010 (2010).

[12] Deepak Mishra and Håkan Johansson. 2019. Optimal channel estimation for hybrid energy beamforming under phase shifter impairments. *IEEE Transactions on Communications* 67, 6 (2019), 4309–4325.

[13] Andrew Y Ng, Daishi Harada, and Stuart Russell. 1999. Policy invariance under reward transformations: Theory and application to reward shaping. In *ICML*, Vol. 99. 278–287.

[14] Vladimir Poulkov, Pavlina Koleva, Oleg Asenov, and Georgi Iliev. 2014. Combined power and inter-cell interference control for LTE based on role game approach. *Telecommunication Systems* 55, 4 (2014), 481–489.

[15] Vishnu V Ratnam, Andreas F Molisch, Ozgun Y Bursalioglu, and Haralabos C Papadopoulos. 2018. Hybrid beamforming with selection for multiuser massive MIMO systems. *IEEE Transactions on Signal Processing* 66, 15 (2018), 4105–4120.

[16] M Series. 2009. Guidelines for evaluation of radio interface technologies for IMT-Advanced. *Report ITU* 638 (2009), 1–72.

[17] M Series. 2017. Guidelines for evaluation of radio interface technologies for IMT-2020. (2017).

[18] Meryem Simsek, Mehdi Bennis, and Ismail Güvenç. 2014. Learning based frequency-and time-domain inter-cell interference coordination in HetNets. *IEEE Transactions on Vehicular Technology* 64, 10 (2014), 4589–4602.

[19] Beatriz Soret, Klaus I Pedersen, Niels TK Jørgensen, and Víctor Fernández-López. 2015. Interference coordination for dense wireless networks. *IEEE Communications Magazine* 53, 1 (2015), 102–109.

[20] Shu Sun, Theodore S Rappaport, Timothy A Thomas, Amitava Ghosh, Huan C Nguyen, István Z Kovács, Ignacio Rodriguez, Ozge Koymen, and Andrzej Partyka. 2016. Investigation of prediction accuracy, sensitivity, and parameter stability of large-scale propagation path loss models for 5G wireless communications. *IEEE Transactions on Vehicular Technology* 65, 5 (2016), 2843–2860.

[21] Richard S Sutton and Andrew G Barto. 2018. *Reinforcement learning: An introduction*. MIT press.

[22] Eric Wiewiora. 2003. Potential-based shaping and Q-value initialization are equivalent. *Journal of Artificial Intelligence Research* 19 (2003), 205–208.

[23] Hailu Zhang, Minghui Min, Liang Xiao, Sicong Liu, Peng Cheng, and Mugen Peng. 2018. Reinforcement learning-based interference control for ultra-dense small cells. In *2018 IEEE Global Communications Conference (GLOBECOM)*. IEEE, 1–6.

[24] Xiaoguang Zhao, Elena Lukashova, Florian Kaltenberger, and Sebastian Wagner. 2019. Practical hybrid beamforming schemes in massive mimo 5g nr systems. In *WSA 2019; 23rd International ITG Workshop on Smart Antennas*. VDE, 1–8.

[25] Xudong Zhu, Zhaocheng Wang, Linglong Dai, and Chen Qian. 2015. Smart pilot assignment for massive MIMO. *IEEE Communications Letters* 19, 9 (2015), 1644–1647.

A AUTHORS BACKGROUND

Aidong Yang

Aidong Yang received the Ph.D. degree in wireless communications from the Dalhousie University, Halifax, NS, Canada, in 2017. His research interests include wireless techniques, 5G communications, machine learning and its applications. He has authored and co-authored over 20 journal and conference papers.

Xinlang Yue

Xinlang Yue received the M.S. degree in Applied Mathematics from Columbia University, New York, NY, US, in 2020. His research interests mainly focus on reinforcement learning with its applications.

Ye Ouyang

Ye Ouyang, Ph.D., is CTO & Senior Vice President of AsiaInfo Technologies. Dr. Ouyang has distinguished experience in R&D and management in telecommunications industry. Prior to AsiaInfo, Dr. Ouyang has been Verizon Fellow and Senior Manager in Verizon. His research is in the interdisciplinary area of wireless communications, data science, and AI. Dr. Ouyang authored more than 30 academic papers, 40 patents, 10 international standards, and 8 books. Dr. Ouyang obtained a Ph.D. from Stevens Institute of Technology, a Master of Science from Tufts University, another Master of Science from Columbia University, and a Bachelor of from Southeast University.